

# Effects of early low-level lead exposure on human brain structure, organization and functions

K. M. Cecil\*

*Cincinnati Children's Environmental Health Center at Cincinnati Children's Hospital Medical Center, Departments of Radiology, Pediatrics, Environmental Health, University of Cincinnati College of Medicine, Cincinnati, OH, USA*

Advanced neuroimaging techniques offer unique insights into how childhood lead exposure impacts the brain. Volumetric magnetic resonance imaging affords anatomical information about the size of global, regional and subcomponent structures within the brain. Diffusion tensor imaging provides information about white matter architecture by quantitatively describing how water molecules diffuse within it. Proton magnetic resonance spectroscopy generates quantitative measures of neuronal, axonal and glial elements via concentration levels of select metabolites. Functional magnetic resonance imaging infers neuronal activity associated with a given task performed. Employing these techniques in the study of the Cincinnati Lead Study, a relatively homogeneous birth cohort longitudinally monitored for over 30 years, one can non-invasively and quantitatively explore how childhood lead exposure is associated with adult brain structure, organization and function. These studies yield important findings how environmental lead exposure impacts human health.

*Received 8 April 2010; Revised 8 August 2010; Accepted 4 September 2010; First published online 28 September 2010*

**Key words:** brain, exposure, imaging, lead

## Introduction

The association between lead exposure and adverse neuropsychological outcomes has long been recognized, however, despite its established neurotoxicity, there remains an allowance of lead within our society based on its usefulness to certain industries and the expenses associated with remediation. For some, the cognitive and behavioral deficits associated with lead are thought to occur primarily because of other known socio-demographic risk factors that occur in combination with lead exposure. In an attempt to explain these deficits from a neurobiological basis, an innovative approach to examine the effects of lead exposure on the human organ of interest, the brain, has been implemented. This approach employs advanced neuroimaging techniques to examine brain volume, organization and function in participants from the Cincinnati Lead Study (CLS). The CLS cohort provides a well-characterized and relatively homogeneous group of young adults to explore the effects of low-to-moderate levels of childhood lead exposure. This presentation describes the imaging methodologies employed, the findings within the CLS and the significance to environmental health.

### *Lead and imaging: a historic look*

Lead encephalopathy is typically associated with blood lead concentrations greater than 100 µg/dl, but may occur with

levels as low as 70 µg/dl. Case reports from hospitalized adult patients with lead encephalopathy show focal lesions in the basal ganglia, thalami, cerebellum, cortical gray matter and subcortical white matter.<sup>1–4</sup> For lead ‘poisoning’ patients, defined as demonstrating blood lead levels greater than 40 µg/dl, conventional neuroimaging studies often reveal evidence of cerebral edema and demyelination.<sup>5</sup> Childhood lead exposure, with blood lead levels below 40 µg/dl, increases the individual likelihood of impaired cognition and executive function, increased impulsiveness, aggression, juvenile delinquent and subsequent adult criminal behavior.<sup>6–11</sup> However, clinical neuroimaging studies in children with low-to-moderate (up to 40 µg/dl) levels of lead exposure tend to have few specific findings described as characteristic of lead exposure that explain these deficits and adverse behaviors.

## Methods

### *General descriptions of advanced imaging techniques*

Taking a cue from psychiatric studies, non-invasive advanced imaging techniques, such as volumetric magnetic resonance imaging (vMRI), proton magnetic resonance spectroscopy (MRS), diffusion tensor imaging (DTI) and functional magnetic resonance imaging (fMRI) were employed as such approaches were considered likely to provide microscopic information about the brain relating to lead exposure. By examining a relatively large group of individuals with similar socio-economic and sociodemographic features, research efforts could minimize confounding effects and focus primarily on lead exposure. This group and advanced imaging approach affords information

\*Address for correspondence: K. M. Cecil, PhD, Professor, Radiology, Pediatrics, Neuroscience & Environmental Health, Cincinnati Children's Hospital Medical Center, Department of Radiology, MLC 5033, 3333 Burnet Avenue, Cincinnati, OH 45229, USA.  
(Email kim.cecil@chmcc.org)

not detectable by conventional imaging of individuals in a clinical setting.

Volumetric imaging requires the acquisition of whole brain, contiguous, three-dimensional and high-resolution anatomical imaging data. The determination of volumes can be afforded via manual segmentation of structures (and sub-structures) or alternatively, via voxel-based morphometric analyses of the imaging data. MRI data acquired at a magnetic field strength of 1.5 Tesla (T) was employed for the CLS studies to determine global and regional changes in brain volume upon comparison with childhood blood lead levels using a voxel-based morphometric (VBM) approach.<sup>12</sup> VBM involves normalizing individual structural MRI scans to a standard template to allow voxel-by-voxel comparisons. This independent analysis approach does not rely on manual segmentation of brain structures via operator determination of intrinsic imaging contrast for structure boundaries. It does not require hypothesized *a priori* regions of involvement. Thus, for an exploratory study, the technique can be quite powerful. Voxel-by-voxel comparisons can be modeled with lead exposure and sociodemographic variables, such as birth weight, maternal socio-economic status (SES), maternal IQ, etc.

MRS acquired within the setting of an MRI examination provides an *in vivo* measure of chemical constituents in localized regions of the brain at concentration levels on the order of 1 to 10 mM. Concentrations of N-acetyl aspartate (NAA), creatine and phosphocreatine (Cr), phosphocholines and glycerolphosphocholine (Cho), myo-inositol (mI), glutamate (Glu) and glutamine (Gln) to form a composite peak referred to as Glx, are determined in each individual spectrum. These chemicals provide information regarding neural integrity via markers of cellular energetics, neuronal, axonal, glial and myelin functioning. For the CLS studies, multiple single volume elements (voxels), each approximately 8 cc in volume, were acquired within medial frontal gray matter, frontal white matter, parietal white matter, temporal lobe, basal ganglia, cerebellar hemisphere (gray and white matter) and cerebellar vermis, respectively, and spectra acquired from these regions.

DTI, a more recently developed MRI technique, affords sensitive microscopic evaluation of water diffusion properties within brain white matter. The DTI acquisition covers the entire brain. However, owing to the nature of the echo planar imaging (EPI) technique, significant distortions occur in the cerebellum that limits its utility for that region. Four key parameters are calculated to describe the water diffusion properties. Water diffusion occurs parallel to axonal fiber tracts as diffusion is restricted in the direction perpendicular to the fiber direction.<sup>13</sup> This directional restriction is thought to arise from the tight, parallel packing of axonal fibers, and is considered to be a measure of white matter tissue organization.<sup>13</sup> Fractional anisotropy (FA) values reflect the degree of directional restriction of water diffusion with values ranging from 0 for isotropic (unrestricted, disorganized) to 1 for anisotropic (restricted, highly organized). A loss of directional

coherence via reduced FA values indicates disorganization of white matter fibers in adults. Mean diffusivity (MD) values measure the mean distance of water diffusion in all directions, which is restricted by white matter fibers, macromolecules and cell membranes. MD values express a measure of cellular integrity and structure with *increasing* MD values indicating loss of microstructure organization.<sup>14</sup> The water can diffuse out more freely as barriers are damaged or destroyed. Axial diffusivity (AD) describes diffusion parallel to the fiber direction and yields information regarding axonal integrity and structure with *decreases* noted in animal models of optic nerve ischemia and multiple sclerosis.<sup>15–17</sup> Radial diffusivity (RD) describes diffusion perpendicular to the fiber direction, and informs about myelin sheath thickness and organization.<sup>18–21</sup> Higher RD values represent *less* myelination or diminished oligodendroglial integrity as more water diffusion occurs perpendicular to the axonal fiber tracts. The combination of FA, MD, AD and RD analyses conducted within a General Linear Model (GLM) allows for sensitive, quantitative, non-invasive, *in-vivo* assessment of white matter architecture of an adult population with significant childhood lead exposure.

fMRI affords an indirect measure of neural activity in the brain by determining regional changes in blood flow related to task, such as thought, experience or action. A verb generation task involves the auditory presentation of a series of nouns. The subject is required to generate verbs that are associated with each noun. For example, if the noun 'ball' is presented as an auditory cue, the subject might generate the verbs 'throw', 'kick' and 'hit'. The subject is instructed to think the verbs silently, without saying them, in order to minimize the motion artifact associated with speech. This expressive task is assumed to require the engagement of dominant frontal lobe and parietal lobe language areas. For the overall study design, the images allowing coverage over the whole brain are acquired with a rapid EPI sequence while the task is repeated multiple times. The fMRI data is first post-processed with a GLM to relate the time series with brain activation on a pixel-by-pixel basis. For each subject, a Pearson's correlation coefficient is calculated for each voxel and then a *z*-score was derived from the coefficient by Fisher's *z*-transformation. During the group analysis, a one-sample *t*-test is performed for each pixel across all subjects to test the significance of the pixel in the group. After transforming *t*-statistics to *z*-score, a statistical parametric map (composite *z*-score map) can be generated to identify brain regions with the most significant contrast between the active task and control task for the entire group. Cluster size and nominal *z*-value can be derived from Monte Carlo simulations using a corrected  $P < 0.001$  to improve specificity and adjust for the inflated  $\alpha$  from multiple comparisons. A random-effect group analysis can be used to test the association between signal activation and parameter of interest. Other potential covariates will also be included in the model in a sequential manner to determine their impact.

### Project oversight

The Institutional Review Boards of the Cincinnati Children's Hospital Medical Center and the University of Cincinnati approved the imaging study protocols. A Certificate of Confidentiality for the overall CLS imaging project was obtained from the National Institutes of Health.

### Summary of imaging parameters within the CLS imaging project

The imaging acquisition parameters for the methods used in the CLS imaging project are summarized in Table 1. Additional details about the image post-processing and analytical models are described within the respective articles.<sup>23–27</sup>

### Cincinnati lead study: characteristics of the cohort

Researchers at the University of Cincinnati designed a longitudinal birth cohort study to evaluate the effects of environmental lead exposure. The CLS, a birth cohort recruited from 1979 to 1984, enrolled women who lived in urban, inner-city neighborhoods with historically high rates of childhood lead poisoning. Women were excluded if they were known to be addicted to drugs, diabetic, or had any known neurological or psychiatric malady. Infants were *excluded* if their birth weight was <1500 g or if genetic or other serious medical issues were present at birth. This process netted 305 newborns who were followed-up quarterly through age at 5 years, semi-annually from age 5 to age 6.5 years, again at age 10 years, and also between the ages of 15–17 years. One hundred and ninety-four CLS subjects between the ages of 19 and 24 years were recruited for the primary imaging study. Thirty-three subjects were excluded from the MRI examination due to the following: too large to fit into the MRI scanner ( $n = 8$ ), failure to appear for the appointment ( $n = 7$ ), pregnant ( $n = 6$ ), refused due to claustrophobia ( $n = 6$ ), non-removable metal in their body ( $n = 5$ ) and unable to give informed consent due to cognitive disability ( $n = 1$ ). Two participants diagnosed with fetal alcohol syndrome as children participated in the imaging and spectroscopy session, but their data is not included in the analyses. Consistent with previous research in this cohort, we found no demographic biases associated with exclusion of these members from the analyses. For the MRS studies, data from 159 participants were included, however for the VBM analyses, motion artifacts resulted in only 157 CLS participants included in the results. A 45 member, representative subset of the 159 CLS participants completed fMRI. In a subsequent evaluation, approximately 100 CLS members participated in a DTI study.

The participants' mothers were enrolled to allow monitoring of blood lead levels for the participants prenatally, at birth, every 3 months to 60 months of age, and every 6 months from 60 to 78 months of age. The arithmetic mean of 23 childhood blood lead assessments for each participant

**Table 1.** Imaging acquisition parameters for methods employed in the CLS Imaging Project

Method	Scanner vendor		Scanner type		Field strength (T)		Pulse sequence		TE (ms)	TR (ms)	FOV (cm)	Matrix	Slice thickness (mm)		Other
Volumetric	General Electric		Signa LX		1.5		IR SPGR	5	12	24 × 19.2	256 × 192		1.5	124 slices	
Spectroscopy	General Electric		Signa LX		1.5		PROBE-PRESS	35	2000	NA	NA		20	8 cc voxel	
Functional	Brucker		Biospec		3.0		GE EPI	38	3000	25.6 × 25.6	64 × 64		5		
Diffusion	Siemens		Trio		3.0		SE EPI	87	6000	25.6 × 25.6	128 × 128		2	$b = 1000 \text{ s/mm}^2$ ; 12 directions	

CLS, Cincinnati Lead Study; TE, echo time; TR, repetition time; FOV, field of view; IR SPGR, inversion recovery spoiled gradient echo; PROBE-PRESS, proton brain examination point resolved spectroscopy; GE EPI, gradient echo echo planar imaging; SE EPI, spin echo echo planar imaging.

collected between 3 and 78 months of life was employed for comparison analyses. The means of childhood blood lead concentrations were previously reported as representative of exposure.<sup>9,22</sup> When no blood lead data were obtained from a given time point, the missing values were imputed from a weighted average of a within-individual regression of blood lead on age and the cohort mean at each age. This imputation was performed to avoid simply excluding those participants who may have one or only a few missing blood lead values in the context of an otherwise data-rich exposure history. Analyses demonstrated that there were no significant differences in magnitude, direction or statistical significance of blood lead regression coefficients when observed and imputed data sets were compared with observed-only data sets. During the first 5 years of life, at least one of the quarterly blood lead assessments exceeded 10  $\mu\text{g}/\text{dl}$  for 99% of the CLS cohort. The peak lead exposure occurred between 2 and 3 years of age for the participants. By adolescence, the mean blood lead levels for the cohort were 2.8  $\mu\text{g}/\text{dl}$  (S.D. 1.3).

## Results

### *Findings from volumetric imaging analyses of the CLS*

Volumetric imaging affords information about the volume of the whole brain, the tissue classes (gray matter, white matter and cerebrospinal fluid (CSF)) and the smaller subcomponent regions. For the CLS VBM analysis, multiple regression models of volume for each tissue class and mean childhood blood lead as the covariate of interest were developed.<sup>23</sup> A simple regression analysis identifies where brain volume change is associated with lead dose. The data was examined for evidence of volume changes in both directions: gain and loss. Owing to the numerous factors involved in brain development that could change composite and regional brain volumes, multiple variables for inclusion in the regression models were evaluated. These variables have also been implicated as alternative and/or additive factors responsible for the cognitive and behavioral manifestations attributed to lead dose. Variables considered include the following: participant age at time of imaging, current marijuana use (obtained from a urine drug screening collected at time of imaging), sex, birth weight, gestational age at birth, maternal IQ, maternal alcohol consumption during pregnancy, maternal marijuana use during pregnancy, maternal tobacco use during pregnancy, mean childhood Hollingshead SES score, current SES score, and home environment (using the mean home observation for measurement of the environment (HOME) score measured in early childhood. After adding an individual putative confounder variable into the otherwise simple linear regression between volume and mean childhood blood lead concentration, the change of regression coefficient ( $\beta$ ) was calculated to evaluate the influence of the variable. This testing was conducted within the regions of interest (ROI) significantly correlated (unadjusted  $P \leq 0.001$ , 700 voxel cluster threshold)

with the mean childhood blood lead concentration. The variable was considered significant and retained for the subsequent final multivariate analysis if adding the variable caused  $>20\%$  of the pixels for the composite ROIs to have over a 10% change in the  $\beta$ -values. Two variables, age at time of imaging and birth weight, satisfied the criteria for inclusion and were included in the final multiple regression model. The effect of sex on lead-associated volumetric changes was assessed by testing for a sex-by-lead interaction in the whole cohort as well as in separate analyses for males and females.

Higher mean childhood blood lead concentrations were associated with significant decrements in gray matter volume for several cortical regions. The voxel-based morphometric analysis revealed an inverse, linear dose–effect relationship between mean childhood blood lead concentration and brain volume in specific regions. Prefrontal cortical areas of lead-related volumetric decline involved the medial and the superior frontal gyri, which include the ventrolateral prefrontal cortex as well as the anterior cingulate cortex (ACC). Other areas of lead-associated volume loss were in postcentral gyri, the inferior parietal lobule and the cerebellar hemispheres. Using conservative, minimum contiguous cluster size and statistical criteria (700 voxels, unadjusted  $P < 0.001$ ), approximately 1.2% of the total gray matter was significantly and inversely associated with mean childhood blood lead concentration. No significant volume changes were observed within white matter or CSF volume.

The effects of yearly mean blood lead from 1 to 6 years of age were also investigated on adult gray matter volume in a voxel-based morphometric analysis of high-resolution volumetric MR images.<sup>24</sup> Later ages of blood lead assessment were found to be more strongly associated with gray matter volume loss than earlier ages of assessment, and that males were more affected than females at all ages. These findings were most prominent in the frontal lobes. The largest regions of gray matter volume loss were found in males associated with mean blood lead levels measured during the 5th and 6th year of life. Although maximum blood lead measures were recorded at approximately 2 years of age, the strongest associations with adult gray matter volume were observed in association with blood lead levels measured at 5 and 6 years of age. These results suggest that blood lead measurements obtained early in childhood, mean or maximum blood lead levels may not fully represent the extent of lead-associated gray matter changes observed in young adults.

### *Findings from MRS analyses of the CLS*

The relationship between brain metabolite levels obtained from MRS analyses in seven brain regions with mean childhood blood lead level were investigated (Fig. 1a).<sup>25</sup> The metabolites examined included NAA, Cr, Cho, mI and Glx (Fig. 1b). Recognizing that other variables could influence the association between metabolite levels and blood lead, the impact of covariates on this relationship were also examined

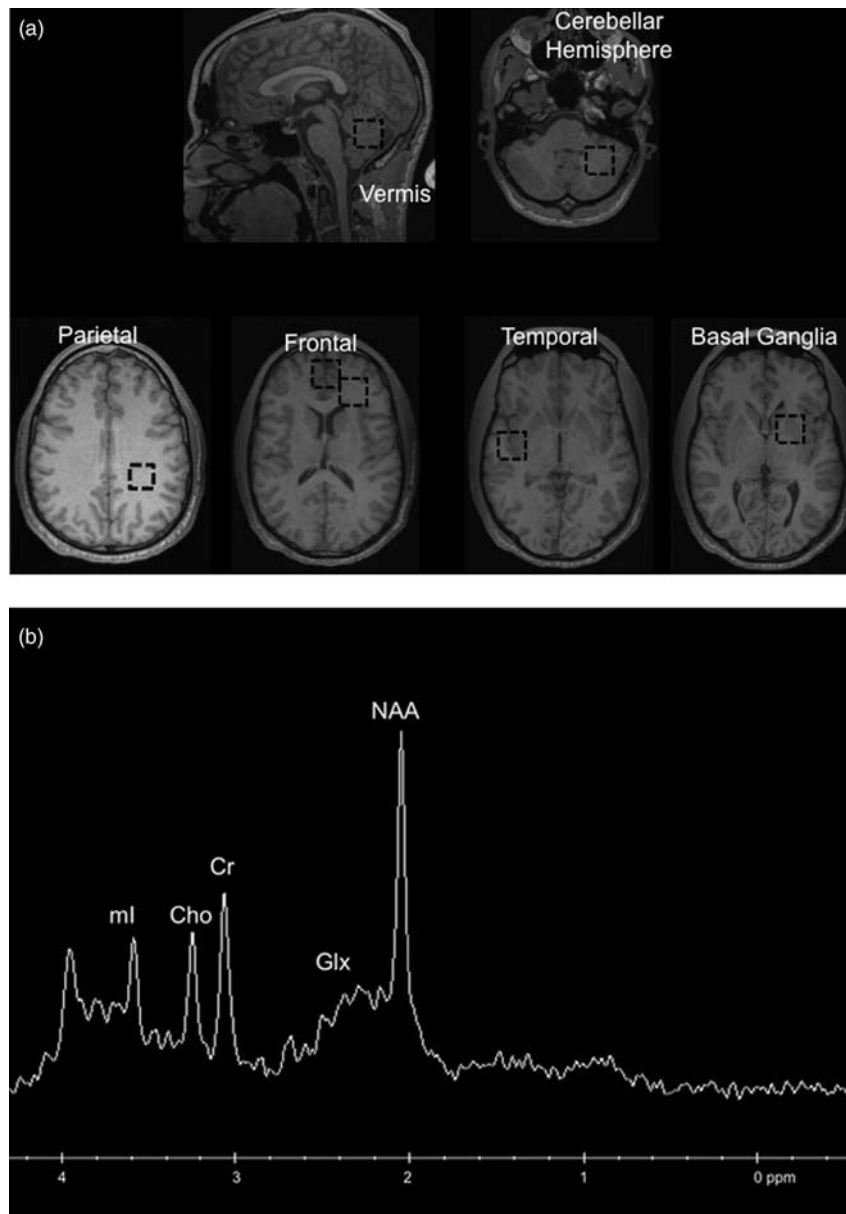


**Fig. 1.** (a) The brain regions sampled by proton MR spectroscopy are indicated on cross-sectional axial slices with black boxes illustrating the approximate locations of the MRS volumes of interest. (b) An example of a proton spectrum obtained from a Cincinnati Lead Study participant sampling the gray matter of the frontal lobe. Metabolite resonances are labeled with NAA for N-acetyl aspartate, Glx for glutamate and glutamine, Cr for creatine, Cho for choline, ml for myo-inositol.

by analyzing the bivariate relationship of the potential covariate with mean childhood blood lead level in each of the sampled brain regions. Variables that could potentially contribute included participant age at time of imaging, full-scale intelligence quotient (FSIQ), current marijuana use (obtained from a urine drug screening collected at time of imaging), sex, birth weight and gestational age. Covariates that were independently related to the outcome in one or more region at  $P < 0.10$  level were included in the subsequent multiple linear regression analyses.<sup>25</sup>

Higher mean childhood blood lead levels adjusted for the impact of age at the time of imaging and FSIQ were associated with lower metabolite concentrations in the left frontal white matter, left parietal white matter, left basal ganglia, left cerebellar hemisphere and vermis.<sup>25</sup>

For gray matter structures, increases in the mean childhood blood level correlated with a decline of the NAA concentration level ( $P = 0.02$ ) and the Cr concentration level ( $P = 0.01$ ) in the basal ganglia, a reduction of NAA ( $P = 0.05$ ) and Cho ( $P = 0.04$ ) concentration levels in the cerebellar hemisphere and

a reduction of Glx ( $P = 0.02$ ) concentration level in the vermis. For white matter regions, reductions of Cho ( $P = 0.02$ ) and Glx ( $P = 0.02$ ) concentration levels in parietal lobe and Cho ( $P = 0.02$ ) in frontal lobe were observed with increasing mean lifetime blood lead concentrations.<sup>25</sup>

### Findings from DTI analyses of the CLS

With the spectroscopy studies indicating metabolic changes, specifically choline in white matter regions sampled, the long-term impact of childhood lead exposure on white matter integrity in the young adults of the CLS was studied using DTI. An inverse association between FA and mean childhood blood lead levels was diffusely observed scattered among white matter regions, including the internal capsule, anterior and superior corona radiata.<sup>26</sup> MD values exhibited both inverse and direct correlations with mean childhood blood lead levels; the primary inverse relationship observed in the corpus callosum, while the primary direct relationship noted in the superior corona radiata.<sup>26</sup> AD values within the anterior and superior corona radiata were inversely correlated with mean childhood blood lead levels, with a small focus of direct association found within the body of the corpus callosum.<sup>26</sup> Finally, both inverse and direct correlations between RD and mean childhood blood lead levels were observed with the primary inverse relationship observed in the corpus callosum, and internal capsule, while the direct relationship noted in the superior corona radiata.<sup>26</sup>

### Findings from fMRI analyses of the CLS

Cognitive and behavioral assessments of individuals exposed to lead have demonstrated adverse changes in brain function. Adults recruited from the CLS underwent an fMRI protocol employing a semantic language task.<sup>27</sup> After adjusting for the confounding factors of birth weight and marijuana usage, the activation in left frontal cortical areas, adjacent to Broca's area and left middle temporal gyrus including Wernicke's area, demonstrate a significant inverse correlation with mean childhood blood lead levels (partial  $R = -0.33$ ,  $P < 0.05$ ; partial  $R = -0.31$ ,  $P < 0.05$ , respectively); while the activation in the right hemisphere homolog of Wernicke's area displays a positive correlation (partial  $R = 0.35$ ,  $P < 0.03$ ).

### Discussion

Experimental animal and *in vitro* models of exposure reveal lead's toxicity to neurons and glia through various mechanisms. Toscano and Guilarte devised a conceptual framework illustrating the effects of developmental lead exposure at glutamatergic synapses and associated signal pathways.<sup>28</sup> Experimental models of developmental lead exposure find a reduced number of synaptic N-methyl-D-aspartate (NMDA) excitatory amino acid receptors (NMDAR). Lead may act as a calcium analog in neurons with exposure inhibiting glutamate

release through binding to the NMDA receptor in an age-dependent and region specific manner, which could produce functional differences despite uniform concentrations within the brain.<sup>29</sup> Volumetric analyses of whole brain magnetic resonance imaging data revealed significant decreases in gray matter volume associated with childhood blood lead concentrations. Affected regions include the portions of the prefrontal cortex and ACC responsible for executive functions, mood regulation and decision-making. These neuro-anatomical findings were more pronounced for males suggesting that lead-related atrophic changes have a disparate impact across genders. The adverse cognitive, and behavioral outcomes may be related to lead's effect on brain development producing persistent alterations in anatomical brain structure. Further analyses demonstrated the blood lead concentrations obtained during later childhood demonstrate greater loss in gray matter volume than childhood mean or maximum values. The MRS study demonstrated an inverse association between mean childhood blood lead levels and metabolic concentrations in five of the seven sampled regions. In gray matter regions sampled, such as the basal ganglia, associations between mean childhood blood lead, NAA and Cr suggest dysfunctional neuronal elements. Changes in frontal and parietal white matter choline concentration levels associated with mean childhood blood lead indicated alterations in the myelin architecture.

Lead alters white matter via expression of genes essential to myelin formation,<sup>30,31</sup> delayed myelin accumulation,<sup>32,33</sup> delayed differentiation of oligodendrocyte progenitors,<sup>34</sup> disordered oligodendrocyte architecture,<sup>35,36</sup> structural changes within the myelin sheath and disintegration of the multilamellar structure<sup>35</sup> and astrogliosis.<sup>37-39</sup> In exposing the immature rat brain to prolonged lead exposure, Struzynska demonstrated glial cell activation occurs with the elevation of GFAP and S-100b proteins, accompanied by increased cytokine production and evidence of axonal damage.<sup>39</sup> With such experimental evidence, one would expect damage to white matter in association with lead exposure in humans. In adjusted DTI analyses, mean childhood blood lead levels were associated with decreased FA throughout white matter suggesting diffuse disorganization. With the additional quantitative measures afforded by DTI, two patterns of injury were observed. The first is a classical injury pattern (low FA, high MD, low AD and high RD) indicating involvement of both the axonal and myelin constituents of white matter. The corona radiata is a later myelinating structure requiring prolonged maturation of cortical connections. The fetal and childhood lead exposure for this later-developing structure produces adverse effects to both axonal and myelin units. In contrast, the second is an unusual pattern (low MD, low RD) with the corpus callosum and internal capsule demonstrating evidence of altered, and perhaps *increased* myelination without significant axonal involvement. The corpus callosum and internal capsule, particularly the posterior limb, are structures whose myelination begins in utero and is usually completed

within the first year of post-natal life. The relative early completion of myelination may afford axonal protection and some measure of adaptation for these structures in response to elevated lead exposures.

fMRI also suggests patterns of injury and compensatory activity associated with childhood lead exposure. For the left inferior and middle frontal gyri (BA46, 47, 9, 10), adjacent to the region including the traditional Broca's area, and the left middle temporal gyrus (BA21), a region involved in language and auditory processing, activation levels are inversely correlated to mean childhood blood lead levels with adjustment for significant confounders, birth weight and marijuana usage. Activation levels of the right superior/middle temporal gyri (BA22, 42) contra lateral to the traditional Wernicke's area, a region regarded responsible for speech perception, are positively correlated with mean childhood blood lead levels with adjustment for significant confounders.

The strong inverse correlation of the mean childhood blood lead levels with brain activation in left frontal cortex and left middle temporal gyrus suggested a damaging effect to the traditional language areas caused by sustained early childhood lead exposure. The negative impact is more severe if the subject had higher mean childhood blood lead levels. Lead exposure during early childhood disrupts the normal brain neural circuitry and exerts a long-term impact on language organization. The positive correlation observed between the mean childhood blood lead levels with the brain activation in the right temporal areas suggests a necessary compensation mechanism for recruiting 'new' areas, contralateral to typical Wernicke's area in this case, for the reduced 'capacity' in the left hemisphere associated with lead exposure. The neuroplasticity observed strongly supports established understanding about language function reorganization, that is, the brain is able to compensate for injury to regions that are structurally and functionally dedicated to language by recruiting support from other cortical regions. However, increased compensation does not necessarily yield equivalent clinical performance.

## Conclusions

The advanced imaging studies of the CLS provide novel insight into explaining the detrimental and permanent effects of childhood lead exposure. The advanced neuroimaging investigations of the adult CLS demonstrated structural, organizational and functional changes in the brain associated with mean childhood blood lead levels. These quantitative imaging outcomes demonstrated diffuse and focal regions of injury and the brain's attempt to provide functional compensation. The brain regions implicated in these studies correspond with the key areas responsible for regulating behavior. The CLS population experienced both focal periods of significant lead exposure and chronic low-to-moderate levels of exposure during their childhood. Thus, it remains uncertain how much, for how long and when lead exposure

produced injury to the brain. Future neuroimaging investigations will be able to recruit populations with low levels of exposure (<10 µg/dl) to further investigate thresholds of exposure producing injury.

## Acknowledgments

This work was supported by grants from the National Institutes of Health, NIEHS P01 ES011261, NIEHS R01 ES015559, NIEHS R21 ES013524, NCI R01 CA112182, M01 RR08084 and the Environmental Protection Agency R82938901.

## Statement of Interest

None.

## References

1. Al Khayat A, Menon NS, Alidina MR. Acute lead encephalopathy in early infancy – clinical presentation and outcome. *Ann Trop Paediatr.* 1997; 1, 39–44.
2. Atre AL, Shinde PR, Shinde SN, *et al.* Pre- and posttreatment MR imaging findings in lead encephalopathy. *AJNR Am J Neuroradiol.* 2006; 27, 902–903.
3. Mani J, Chaudhary N, Kanjalkar M, Shah PU. Cerebellar ataxia due to lead encephalopathy in an adult. *J Neurol Neurosurg Psychiatr.* 1998; 65, 797.
4. Tuzun M, Tuzun D, Salan A, Hekimoglu B. Lead encephalopathy: CT and MR findings. *J Comput Assist Tomogr.* 2002; 26, 479–481.
5. Staudinger KC, Roth VS. Occupational lead poisoning. *Am Fam Physician (Review)* 1998; 57, 719–726.
6. Bellinger DC, Stiles KM, Needleman HL. Low-level lead exposure, intelligence and academic achievement: a long-term follow-up study. *Pediatrics.* 1992; 90, 855–861.
7. Canfield RL, Gendle MH, Cory-Slechta DA. Impaired neuropsychological functioning in lead-exposed children. *Dev Neuropsychol.* 2004; 26, 513–540.
8. Canfield RL, Henderson CR Jr, Cory-Slechta DA, *et al.* Intellectual impairment in children with blood lead concentrations below 10 microg per deciliter. *N Engl J Med.* 2003; 348, 1517–1526.
9. Dietrich KN, Berger OG, Succop PA, Hammond PB, Bornschein RL. The developmental consequences of low to moderate prenatal and postnatal lead exposure: intellectual attainment in the Cincinnati lead study Cohort following school entry. *Neurotoxicol Teratol.* 1993; 15, 37–44.
10. Needleman HL, Gatsonis CA. Low-level lead exposure and the IQ of children. A meta-analysis of modern studies. *JAMA.* 1990; 263, 673–678.
11. Wright JP, Dietrich KN, Ris MD, *et al.* Association of prenatal and childhood blood lead concentrations with criminal arrests in early adulthood. *PLoS Med.* 2008; 5, e101.
12. Ashburner J, Friston KJ. Voxel-based morphometry – the methods. *Neuroimage.* 2000; 11, 805–821.
13. Le Bihan D, Mangin JF, Poupon C, *et al.* Diffusion tensor imaging: concepts and applications. *J Magn Reson Imaging.* 2001; 13, 534–546.

14. Beaulieu C. The basis of anisotropic water diffusion in the nervous system – a technical review. *NMR Biomed.* 2002; 15, 435–455.
15. Kim JH, Budde MD, Liang HF, *et al.* Detecting axon damage in spinal cord from a mouse model of multiple sclerosis. *Neurobiol Dis.* 2006; 21, 626–632.
16. Kinoshita Y, Ohnishi A, Kohshi K, Yokota A. Apparent diffusion coefficient on rat brain and nerves intoxicated with methylmercury. *Environ Res.* 1999; 80, 348–354.
17. Song S-K, Sun S-W, Ju W-K, *et al.* Diffusion tensor imaging detects and differentiates axon and myelin degeneration in mouse optic nerve after retinal ischemia. *Neuroimage.* 2003; 20, 1714–1722.
18. Partridge SC, Mukherjee P, Henry RG, *et al.* Diffusion tensor imaging: serial quantitation of white matter tract maturity in premature newborns. *Neuroimage.* 2004; 22, 1302–1314.
19. Song S-K, Sun S-W, Ramsbottom MJ, *et al.* Dysmyelination revealed through MRI as increased radial (but Unchanged Axial) diffusion of water. *Neuroimage.* 2002; 17, 1429–1436.
20. Song S-K, Yoshino J, Le TQ, *et al.* Demyelination increases radial diffusivity in corpus callosum of mouse brain. *Neuroimage.* 2005; 26, 132–140.
21. Suzuki Y, Matsuzawa H, Kwee IL, Nakada T. Absolute eigenvalue diffusion tensor analysis for human brain maturation. *NMR Biomed.* 2003; 16, 257–260.
22. Dietrich KN, Succop PA, Berger OG, Hammond PB, Bornschein RL. Lead exposure and the cognitive development of urban preschool children: the Cincinnati lead study cohort at age 4 years. *Neurotoxicol Teratol.* 1991; 13, 203–211.
23. Cecil KM, Brubaker CJ, Adler CM, *et al.* Decreased brain volume in adults with childhood lead exposure. *PLoS Med.* 2008; 5, e112.
24. Brubaker CJ, Dietrich KN, Lanphear BP, Cecil KM. The influence of age of lead exposure on adult gray matter volume. *Neurotoxicology.* 2010; 31, 259–266.
25. Cecil KM, Dietrich KN, Altaye M, *et al.* Proton magnetic resonance spectroscopy in adults with childhood lead exposure. *EHP* (in press).
26. Brubaker CJ, Schmithorst VJ, Haynes EN, *et al.* Altered myelination and axonal integrity in adults with childhood lead exposure: a diffusion tensor imaging study. *Neurotoxicology.* 2009; 30, 867–875.
27. Yuan W, Holland SK, Cecil KM, *et al.* The impact of early childhood lead exposure on brain organization: a functional magnetic resonance imaging study of language function. *Pediatrics.* 2006; 118, 971–977.
28. Toscano CD, Guilarte TR. Lead neurotoxicity: from exposure to molecular effects. *Brain Res Rev.* 2005; 49, 529–554.
29. Guilarte TR, Miceli RC, Jett DA. Neurochemical aspects of hippocampal and cortical Pb<sup>2+</sup> neurotoxicity. *Neurotoxicology.* 1994; 15, 459–466.
30. Deng W, Poretz RD. Lead exposure affects levels of galactolipid metabolic enzymes in the developing rat brain. *Toxicol Appl Pharmacol.* 2001; 172, 98–107.
31. Zawia NH, Harry GJ. Exposure to lead-acetate modulates the developmental expression of myelin genes in the rat frontal lobe. *Int J Dev Neurosci.* 1995; 13, 639–644.
32. Toews AD, Blaker WD, Thomas DJ, *et al.* Myelin deficits produced by early postnatal exposure to inorganic lead or triethyltin are persistent. *J Neurochem.* 1983; 41, 816–822.
33. Toews AD, Krigman MR, Thomas DJ, Morell P. Effect of inorganic lead exposure on myelination in the rat. *Neurochem Res.* 1980; 5, 605–616.
34. Deng W, Poretz RD. Protein kinase C activation is required for the lead-induced inhibition of proliferation and differentiation of cultured oligodendroglial progenitor cells. *Brain Res.* 2002; 929, 87–95.
35. Dabrowska-Bouta B, Struzynska L, Walski M, Rafalowska U. Myelin glycoproteins targeted by lead in the rodent model of prolonged exposure. *Food Chem Toxicol.* 2008; 46, 961–966.
36. Dabrowska-Bouta B, Sulkowski G, Bartosz G, Walski M, Rafalowska U. Chronic lead intoxication affects the myelin membrane status in the central nervous system of adult rats. *J Mol Neurosci.* 1999; 13, 127–139.
37. Selvin-Testa A, Loidl CF, Lopez-Costa JJ, Lopez EM, Pecci-Saavedra J. Chronic lead exposure induces astrogliosis in hippocampus and cerebellum. *Neurotoxicology.* 1994; 15, 389–401.
38. Struzynska L, Bubko I, Walski M, Rafalowska U. Astroglial reaction during the early phase of acute lead toxicity in the adult rat brain. *Toxicology.* 2001; 165, 121–131.
39. Struzynska L, Dabrowska-Bouta B, Koza K, Sulkowski G. Inflammation-like glial response in lead-exposed immature rat brain. *Toxicol Sci.* 2007; 95, 156–162.